



## THERMAL BEHAVIOR OF FERROCENOYLACETONE BENZOYLHYDRAZONE AND ITS COMPLEX WITH COPPER(II) ION

*Sulaymanova Z. A., Umarov B.B., Kadirova Z.Q.,  
Xudoyarova E.A., Babamurodova N.J.  
Bukhara State University, Bukhara, 200100, Uzbekistan*

### ABSTRACT

*We obtained  $\beta$ -diketone-1-ferrocenibutanedione-1,3 (ferrocenoylacetone) by Claisen condensation. Hydrazone ( $H_2L$ ) of 1-ferrocenylbutanedione-1,3 benzoic acid was synthesized by the reaction of monocarboxylic acid hydrazide with ferrocenoylacetone. On its basis, a complex with a copper(II) ion was obtained. The thermal properties of the resulting ligand, ferrocenoylacetonebenzoylhydrazone and its complex  $CuL \cdot NH_3$ , were studied.*

*From the obtained thermograms it is clearly seen that the most significant weight changes for the ligand - ferrocene derivative - benzoylhydrazoneferrocenoylacetone occur at  $T_{d,max}=260^\circ C$ , when the mass loss rate reaches its maximum value, and for the  $CuL \cdot NH_3$  complex the similar temperature is -  $180^\circ C$ . The activation energies for the  $H_2L$  ligand and its  $CuL \cdot NH_3$  complex were determined to be 36.32 kJ/mol and 5.367 kJ/mol, respectively.*

**Keywords:** *ligand, complex, thermal analysis, derivatogram, activation energy.*

### INTRODUCTION

Ferrocene derivatives, especially  $\beta$ -dicarbonyl compounds, attract the attention of researchers, since such compounds are characterized by a number of important advantages in practical application. The practical significance of these compounds is emphasized by the special role of hydrazone complexes in the composition of antitumor, antiviral, antibacterial, anticarcinogenic and carcinoprotective agents[1–10]. It should be noted that complexes of this class are promising objects for atmospheric nitrogen fixation, direct dissolution of metal derivatives or salts in non-aqueous solvents, stabilization of polymers, and

preparation of new types of combustion regulators and catalysts. The possibility of synthesizing binuclear complexes with 3d-metal ions along with mononuclear ligands based on new ligands predetermines the emergence of new areas of practical use of these compounds [11–22].

## METHODICAL PART

### *Materials and research methods*

**Synthesis of ferrocenoylacetone.** Sodium metal 0.09 g-atom was added in small portions to a solution of ofacetylferrocene 0.09 mol in 150 ml of ethyl acetate with continuous stirring. The reaction mixture was kept for 5-6 hours at a temperature of 40-45°C. The resulting precipitate salt of the sodium derivative of ferrocenoylacetone was introduced into a separating funnel, cooled with ice, added ether and treated with a 10% HCl solution.

The extract after decomposition was dried with  $MgSO_4$ . Then the solvent was distilled off and, upon cooling, a black mass precipitated from the mother liquor, which was treated twice with ethyl ether. After washing, a red powdery precipitate precipitated. The resulting precipitate was filtered off, washed with water, dried, and recrystallized from hexane. Yield: 13.3 g (50.2%), dark red crystals.  $T_m$  - 95-96.5°C. Found, %: C 62.35; H 5.34; About 11.55; Fe 20.76. For  $C_{14}H_{14}FeO_2$  calculated, %: C 62.25; H5.22; About 11.85; Fe 20.68.

**Synthesis of benzoylhydrazonferrocenoylacetone.** To a solution of 0.04 mol of ferrocenoylacetone in 50 ml of absolute alcohol was gradually added 5 0.04 mol of benzoylhydrazide in 100 ml of ethanol. The reaction mixture was heated under reflux for an hour. After removing the solvent, the mother liquor was left for 2 days. The precipitated crystals were filtered off, washed with alcohol, and dried in air. Yield: 9.93 g (65%), dark brown crystals. Found, %: C 64.76, H 5.18, O 8.21, N 7.19, Fe 14.43. Calculated for  $C_{21}H_{20}N_2O_2Fe$ , %: C 64.95, H 5.16, O 8.25, N 7.22, Fe 14.43.

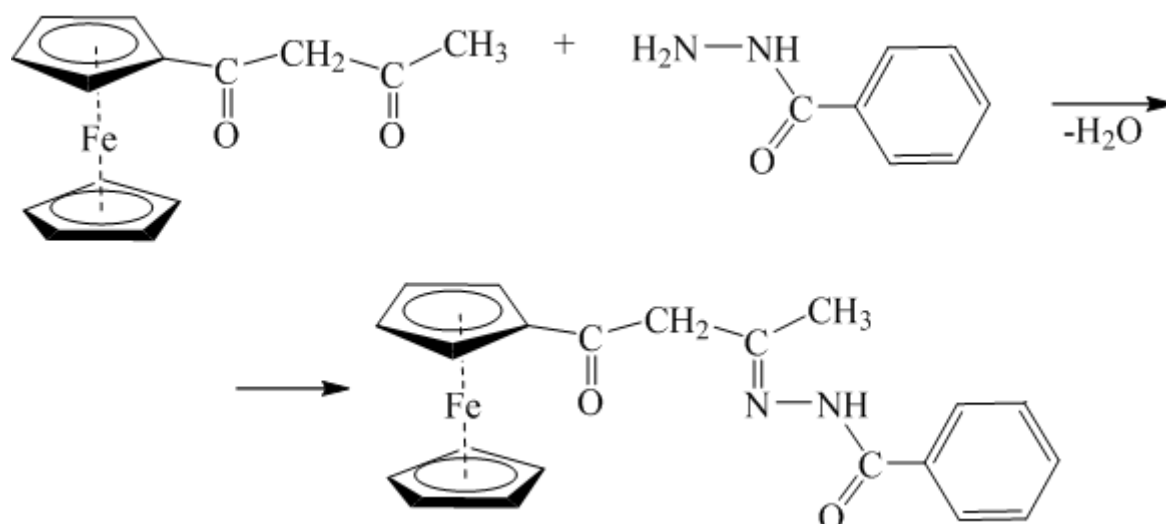
**Synthesis of copper(II) complex of benzoylhydrazonferrocenoylacetone.** To a hot solution of 0.005 mol of

ferrocenoylacetonebenzoylhydrazone in 50 ml of ethanol was added with stirring 0.005 mol of copper (II) acetate in 50 ml of concentrated ammonia. After 3 days, the precipitate formed was separated, washed thoroughly with water, and dried. Yield: 64%. Found, %: C 53.75, H 4.78, O 6.81, N 9.1, Fe 11.97, Cu 13.62. Calculated for  $C_{21}H_{21}N_3O_2FeCu$ , %: C 53.96, H 4.5, O 6.85, N 8.99, Fe 12, Cu 13.7.

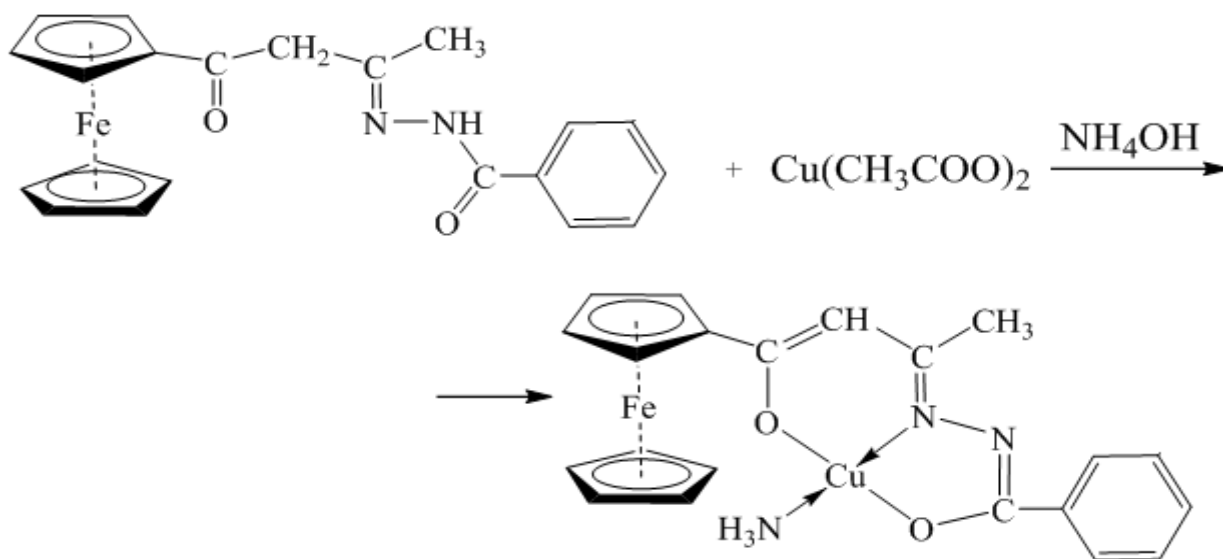
## RESULTS AND DISCUSSIONS

We obtained ferrocenoylacetone (1-Ferrocenylbutanedione-1,3) from monoacetylferrocene (MAF) by Claisen ester condensation [23-25].

Ferrocene $\beta$ -diketonehydrazone was obtained by reacting an alcoholic solution of hydrazide and  $\beta$ -diketone in a 1:1 molar ratio.



The interaction of an alcoholic solution of ferrocenoylacetonebenzoylhydrazone and an aqueous ammonia solution of copper(II) acetate in a ratio of 1:1 yielded the  $CuL \cdot NH_3$  complex.



The study of the composition and structure of the synthesized ligands and coordination compounds was supplemented by taking their thermograms. Absolutely all synthesized complexes are high-melting substances with  $T_m \geq 130^\circ\text{C}$ . In the structure of compounds synthesized by us, the presence of a ferrocene fragment makes it difficult to detect melting temperatures and phase transitions, because all the synthesized derivatives of ferrocene are colored, and upon heating, such coloring intensifies. It is quite difficult to use normal methods to fix the beginning and end of the phase transition.

Thermal analysis was performed by thermogravimetry (TG), derivative thermogravimetry (DTG) and differential thermal analysis (DTA) on a complex thermal analytical unit "DERIVATOGRAPH" of the Paulik-Paulik-Erdey system of the MOM company (Hungary) in dynamic mode with a heating rate of 8,8 deg/min in a stationary air atmosphere in the temperature range from room temperature to  $800^\circ\text{C}$  in platinum crucibles. The weighed portions were 40–100 mg. The inert substance is calcined aluminum oxide ( $\text{Al}_2\text{O}_3$ ).

When performing quantitative calculations of thermal endo- and exo-effects, benzoic acid ( $\Delta H_f = 141.9 \text{ kJ/kg}$ ) was used as a standard for calibration.

The thermograms of these compounds contain curves of temperature changes, the loss of TG mass, its derivative DTG, and the DTA differential thermal analysis curve, which corresponds to the dependence  $(T_{\text{sam}} - T_{\text{et}}) = f(T)$ , here  $T_{\text{sam}}$

is the temperature of the test sample,  $T_{et}$  is the temperature of the standard. Differential thermal analysis (DTA) is a research method that consists in heating or cooling a sample at a certain rate and comparison sample (standard) ( $T_{et}$ ), which does not undergo practically any changes in the observed temperature range.

When performing quantitative calculations of thermal endo- and exoeffects, benzoic acid was used as a standard for calibration ( $\Delta H_f = 141,9$  kJ/kg).

The results of thermal analysis demonstrate, in fact, that thermal decomposition of the  $H_2L$  ligand and its complex compound  $CuL \cdot NH_3$  with copper(II) ions occurs sequentially in several stages, with the burning out of the organic part of the molecule, the simultaneous decomposition of substances, the oxidation of decomposition products and the production of metal oxides.

When considering the thermogram of the  $H_2L$  ligand (Fig. 1) on the DTG curve in the temperature range from room temperature to  $100^\circ C$ , one can see the first stage (temperature region I) of the age. At the beginning of the first stage, relatively moderate changes in thermal curves (DTA, TG, DTG) are observed. Weight loss at the first stage is determined from the TG curve and is 8.3% of the original. Weight loss at this stage can be attributed to decomposition processes, when adsorbed molecules leave the surface and near-surface layers of the sample.

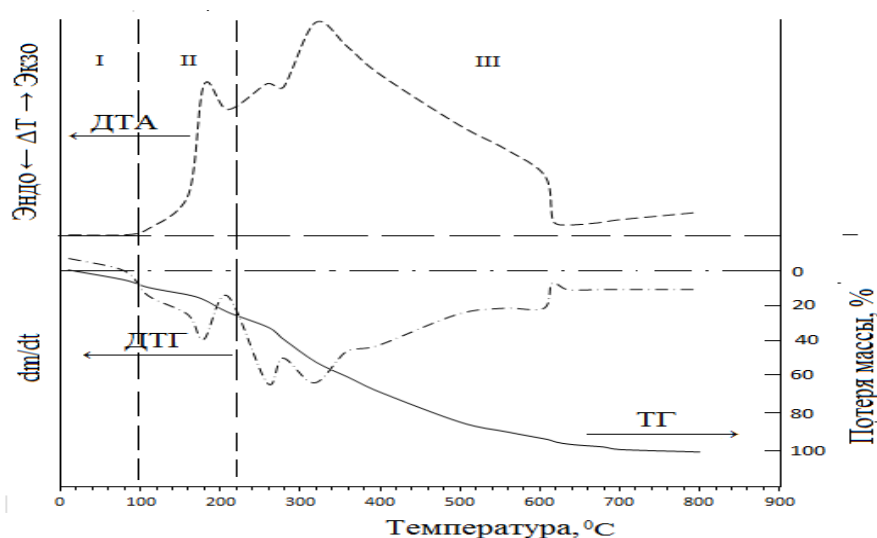


**Fig. 1. Thermogram of benzoylhydrazonferrocenoylacetone.**

Analysis of the  $\text{CuL}\cdot\text{NH}_3$  thermogram (Fig. 2) showed that for the compound, the thermal destruction of the organic part of the molecule starts at  $100^\circ\text{C}$  and ends at  $800^\circ\text{C}$  (Table 1). This process is marked on the DTA curve a number of endo- and exoeffects, caused by the gap of some chemical bonds and the formation of new.

Further, as the temperature rises, the second stage of mass loss in the temperature range  $100 - 220^\circ\text{C}$  is indicated on the DTG curve (temperature region II in Fig. 1). On the thermogram of the ligand in the region of  $100-220^\circ\text{C}$ , endoeffects and a weight loss of up to 20.1% were found, related to the elimination of the apomatic radical from the ligand molecule.

The following curves with an endothermic phenomenon occur as a result of the loss of mass during the destruction of diketone fragments. The thermal scanning area in the temperature interval  $200$  to  $340^\circ\text{C}$  on all two thermograms is characterized by very sharp changes. The DTA curve has the highest elevation angle, which indicates a rapid intensification of thermal oxidizing processes in this temperature range. It is in this range that the TG curve has a sharp decrease, showing the presence of a decrease in the mass of the ligand, and this is immediately reflected on the DTG curve by the appearance of an intense deep peak. The lower extreme point of the peak at  $240^\circ\text{C}$  corresponds to the maximum rate of weight loss. It is likely that, in this case, the bonds are broken and the thermolysis products are oxidized. The weight loss for the second stage is 20.1%, the main part of which falls on the above interval of  $200-340^\circ\text{C}$ . The intensity of the loss clearly exceeds that in comparison with the first stage. The analysis of the thermogravimetry data showed that the mass loss of the two samples studied by us, in general, occurs in three successive stages (Table 1).

The first stage - in the temperature range from  $20$  to  $100 - 120^\circ\text{C}$  is associated with the removal of substances (from 7.8 to 8.3% of the initial mass of the sample), absorbed by samples in the process of adsorption and absorption. The second one, in the temperature range from  $100-120$  to  $220-340^\circ\text{C}$ , is associated

with destruction during oxidative reactions, leading to weight loss from 20.1 to 41%. The third one is in the temperature range from 220–340 to 600–640°C.

The third stage of losses covers the temperature range 340–640°C, due to losses (59.4–70.6%) associated with combustion processes (temperature region III in Fig. 2). For heating curves H<sub>2</sub>L three exothermic effects are observed at 180, 295 and 380°C and two endothermic effects at 195 and 300°C. These thermal effects are associated with stepwise decomposition, combustion, and the formation of end products of ligand thermolysis.

**Table 1**

**Data from the analysis of the parameters of the stages of thermal destruction of the studied samples**

No	Samplename	Temperature range (by stages), °C	The amount of weight loss, %	Temperature of maximum mass loss rate, °C
1	H <sub>2</sub> L	20-120	8,3	100
		100-220	20,1	180
		220-640	70,6	250, 320
2	CuL·NH <sub>3</sub>	20-100	7,8	120
		120-340	41	200, 260
		340-600	59,4	400, 460

A different thermal behavior is observed when the CuL·NH<sub>3</sub> complex is heated (Fig. 2). When considering the thermogram of the CuL·NH<sub>3</sub> complex on the DTG curve in the temperature range from room temperature to 120°C, one can see the first stage (temperature region I) of the mass loss. At the beginning of the first stage, relatively moderate changes are observed thermal curves (DTA, TG, DTG). Weight loss at the first stage is determined from the TG curve and is 7.8% of the original. Weight loss at this stage can be attributed to decomposition processes,

when the solvent molecules leave the surface and near-surface layers of the sample.

Judging by the TGP curve, the thermal decomposition of the complex also occurs in three stages, but unlike the H<sub>2</sub>L ligand, in other temperature ranges:  $\Delta T_1=20-120^\circ\text{C}$ ,  $\Delta T_2=120-340^\circ\text{C}$ ,  $\Delta T_3=340-600^\circ\text{C}$  (Table 1). The same table shows the mass loss in%, the temperature of the maximum loss rate and the magnitude of the maximum loss rate per minute. The DTA curve of CuL·NH<sub>3</sub> shows five exothermic effects at 160, 240, 360, 400, 520°C and six endothermic effects at 140, 220, 280, 380, 480, 600°C. The nature of thermal effects is associated decomposition of the organic part of the complex, combustion of thermal decomposition products, and formation of copper(II) and Fe(II) oxides (Table 2). Thermal decomposition of the ferrocene fragment occurs quite at high temperatures (475-500°C). In the first place, during the thermolysis of metallocene, the dissociation of the C–H bond occurs and hydrogen is the main gaseous decomposition product, and polybination products are included in the composition of solid products.

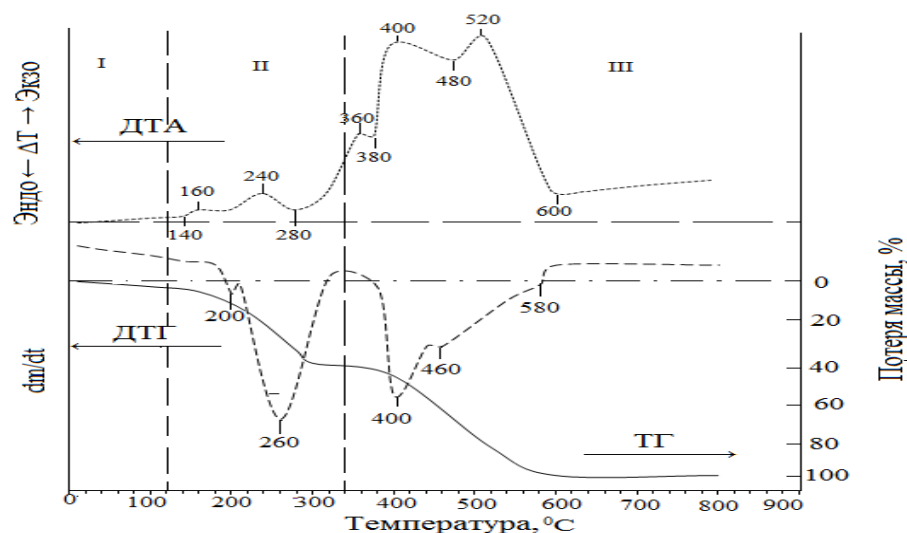


**Fig. 2. Thermogram of the CuL·NH<sub>3</sub> complex.**

Judging by the DTG curve, the thermal decomposition of the complex also occurs in three stages, but, unlike the H<sub>2</sub>L ligand, in other temperature ranges:  $\Delta T_1 = 20 - 100^\circ\text{C}$ ,  $\Delta T_2 = 100 - 220^\circ\text{C}$ ,  $\Delta T_3 = 220 - 640^\circ\text{C}$  (Table 1). The same



table shows the mass loss in%, the temperature of the maximum loss rate and the magnitude of the maximum loss rate per minute.

**Table 2**

**Results of thermal analysis of the synthesized compounds**

Compound	Interval, °C	Peakeffect, °C	The nature of the effect	Weightloss, %
H <sub>2</sub> L	110-202	200	Exothermic	20
	210-220	215	Endothermic	28,3
	221-296	295	Exothermic	48,6
	297-342	340	Endothermic	52.1
	341-385	380	Exothermic	67,6
CuL·NH <sub>3</sub>	130-142	140	Endothermic	6,2
	145-162	160	Exothermic	9,3
	165-222	220	Endothermic	18
	230-245	240	Exothermic	23
	260-290	280	Endothermic	40
	320-362	360	Exothermic	42
	363-380	380	Endothermic	44
	381-405	400	Exothermic	57
	410-485	480	Endothermic	68
	482-522	520	Exothermic	77

Based on the set of available experimental data, it becomes possible to evaluate the thermal stability of the studied objects by two in different ways: the first, according to the characteristic temperatures  $T_{10}$ ,  $T_{20}$ ,  $T_{50}$  and the second, according to the values of the activation energy of the thermal oxidizer destruction (Table 3).

If we evaluate the thermal stability of samples by characteristic temperatures, then as the thermal stability, it can be seen that the thermal stability of the  $\text{CuL}\cdot\text{NH}_3$  complex is higher than that of its  $\text{H}_2\text{L}$  ligand.

According to the thermogravimetric curves, the so-called “inflection points”, that is temperature at which the maximum rate of weight loss occurs for each stage of decomposition under the selected conditions of the dynamic heating regime. The most significant changes in mass for the  $\text{H}_2\text{L}$  ligand occur at  $T_{d,\max}=240^\circ\text{C}$ , and for the  $\text{CuL}\cdot\text{NH}_3$  complex, the analogous temperature is  $-260^\circ\text{C}$ .

An energy assessment of the main exo- and endothermic effects has been made. By numerical processing of thermogravimetric data the values of the activation energy ( $E_a$ ) of destruction for each stage near the “inflection point” were calculated (Table 3).

According to the data of thermal analysis, the values are calculated activation energies, kinetic characteristics, and in particular, reaction orders are most often obtained from thermogravimetry lines with programmable temperature. These results are very useful for making various comparisons, but one should not draw far-reaching conclusions based on them. In most cases, thermal decomposition reactions are very complex processes occurring in several more or less clearly expressed stages. In addition, in the course of the reaction and with an increase in temperature, the physical and chemical properties of the medium change. As a result, the discussed kinetic characteristics, as a rule, do not have a direct relationship with the ongoing main decomposition processes.

**Table 3**

**Comparative results of evaluation of the thermal stability of the studied samples according to the characteristic temperatures and activation parameters**

№	Name sample	Characteristic temperature, °C			Activation energy, kJ/mol	Correlation coefficient, $R^2$	Temperature, °C
		$T_{10}$	$T_{20}$	$T_{50}$			
1	$\text{H}_2\text{L}$	150	230	380	5,367	0,9999	40-60
					18,52	0,9672	330-350

					2,079	0,9983	530-550
2	CuL·NH <sub>3</sub>	230	255	435	36,32	0,9905	100-120
					5,348	0,9365	330-350
					74,94	0,9807	580-600

## CONCLUSION

A comparison of the thermograms (DTA) of the ligand and the complex shows that, if oxidative, and in connection with them, the degradation processes of the ligand are observed within 100 – 340°C, then for the complex, this is observed in a much higher temperature range of 160–520°C, i.e., the intensity of the noted processes is also relatively lower in the case of the ligand. The presence of carbon contamination with residues of the ligand and the Cu(II) complex can be explained by the high stability of these compounds, since they cannot completely decompose up to 1000°C. Carbon residues were found practically in the metal chelate with metal oxides, which can be explained by the high stability of the complex containing the ferrocene derivative. Complexation with a metal increased their stability, so the complex could not decompose completely at high temperatures.

## References

1. Patra M, Gasser G, Wenzel M, Merz K, Bandow JE, Metzler Nolte N. Synthesis and biological evaluation of ferrocene – containing bioorganometallics inspired by the antibiotic platensimycin lead structure // *Organometallics* . - 2010. - Vol. 29. - P. 4312-4315.
2. Morales-Espinoza E.G., Sanchez-Montes E., Klimova E., Klimova T., Lijanovna I.V., Maldonado J.L., Ramos-Ortiz G, Hernandez-Ortega S., Martinez-Garcia M. Dendrimers containing ferrocene and porphyrin moieties: synthesis and cubic non-linear optical behavior // *Molecules*. - 2010. - №15. - P. 2564-2568.

3. Biot C., Glorian G., Maciejewski L.A., Brocard J.S. Synthesis and Antimalarial Activity in Vitro and in Vivo of a New Ferrocene-Chloroquine Analogue // *J. Med. Chem.* -1997. -Vol. 40. - P. 3715-3718.

4. Osella D., Ferrali M., Zanello P., Laschi F., Fontani M., Nervid C., Cavigiolo C. On the mechanism of the antitumor activity of ferrocenium derivatives // *Inorg. Chim. Acta.* - 2000. - Vol. 306. - P. 42-48.

5. Hudson R.D.A. Ferrocene polymers: current architectures, syntheses and utility // *J Organomet Chem.* -2001. - Vol. 637. - P. 47-50.

6. Zheng J, Wu KL, Shi TH, Xu Y. A series of novel ferrocene based dipeptide receptors for electrochemistry and biological activity // *Appl Organometal Chem.* - 2013. - Vol. 27. - P. 698- 704.

7. Gupta S.R, Mourya P, Singh M.M, Singh V.P. Synthesis, structural, electrochemical and corrosion inhibition properties of two new ferrocene Schiff bases derived from hydrazides // *J Organomet Chem.* -2013. - Vol. 767. - P. 136- 140

8. Beer P.D., Smith D.R.J. Tunable bis (ferrocenyl) receptors for the solution phase electrochemical sensing of transition-metal cations // *J Chem Soc Dalton Trans.* -1998. - Vol. 3. - P. 417-420.

9. Van Staveren D.R., Metzler-Nolte N. Bioorganometallic Chemistry of Ferrocene // *Chem. Rev.* - 2004. - Vol. 104. - № 12.- P. 5931-5985.

10. Dive D., Biot C. Ferrocene conjugates of chloroquine and other antimalarials: the development of ferroquine, a new antimalarial // *Chem Med Chem.* - 2008. - Vol. 3. - P. 4678-4682.

11. Top S., Vessieres A., Cabestaing C., Laios I., Leclercq G., Provot C., Jaouen G., Ferrocifens and ferrocifenols as new potential weapons against breast cancer // *J. Organomet. Chem.* - 2018.- Vol. 3. - P. 637-639.

12. Top S., Vessieres A., Leclercq G., Quivy J., Tang J., Vaissermann J., Huche M., Jaouen G. Facile synthesis and strong antiproliferative activity of disubstituted diphenylmethylidene-[3]-ferrocenophanes on breast and prostate cancer cell lines // *Chem. Eur. J.* - 2003. - Vol. 9. - P.5223–5236.

13. Itoh T., Shirakami S., Ishida N., Yamashita Y., Yoshida T., Kim H-S., Wataya Y. Synthesis of novel ferrocenyl sugars and their antimalarial activities // *Bioorg Med ChemLett.* - 2000. - Vol. 10. - P. 1657-1659.

14. Hussain R.A., Badshah A., Sohail M, Lal B., Altaf AA. Synthesis, chemical characterization, DNA interaction and antioxidant studies of ortho, meta and parafluoro substituted ferrocene incorporated selenoureas. // *InorgChimActa.* - 2013. - Vol. 402. - P. 133-139.

15. Hassan A.S., Hafez T.S., Osman S.A., Ali M.M. Synthesis and *in vitro* cytotoxic activity of novel pyrazolo [1,5-*a*] pyrimidines and related Schiff bases // *Turk J Chem.* - 2015. - Vol. 83. - P. 27-39.

16. Abd-ElzaherM.M., Mohamad M.E. Shakdofa, Hanan A. Mousa, Samia A. Moustafa. Synthesis, Characterization and Biological Activity of Some Ferrocenyl Complexes Containing Antipyrine Moiety // *SOP TRANSACTIONS ON APPLIED CHEMISTRY.* -2014. -Vol. 1. -№1.- P. 42-52.

17. Abd-Elzaher M.M. Synthesis, characterization, and antimicrobial activity of cobalt(II), nickel(II), copper(II) and zinc(II) complexes with ferrocenyl Schiff bases containing a phenol moiety // *Appl. Organomet. Chem.* .-2004. -Vol. 18. - №4.- P. 149-155.

18. Ashraf S. Hassan, Taghrid S. Hafez. Antimicrobial Activities of Ferrocenyl Complexes // *Journal of Applied Pharmaceutical Science.* -2018. -Vol. 8. -№5.- P. 156-165. Availableonlineat<http://www.japsonline.com>.

19. Deveci P, Arslanb U. Synthesis of novel ferrocene containing vic-dioxime ligands and their Ni(II), Cu(II) and Co(II) complexes: Spectral, electrochemical and biological activity studies // *J. Organomet Chem.* - 2011. -Vol. 696. - P. 1756 -1763.

20. Ali S., Yasin G, Zuhra Z., Wu Z., Butler IS, Badshah A, Din IU. Ferrocene-based bioactive bimetallic thiourea complexes: synthesis and spectroscopic studies // *Bioinorganic Chemistry and Applications.* - 2015. - Vol. 10. - №8. - P. 3756-3763.

21. Mahmood W.H, Mahmood N.F, Mohamed G.G. Synthesis, physicochemical characterization, geometric structure and molecular docking of new biologically active ferrocene based Schiff base ligand with transition metal ions // *ApplOrganometal Chem.* -2017. - Vol. 848. - №8. - P. 288-301.

22. Chohan Z.H.Synthesis of organometallic-based biologically active compounds: In vitro antibacterial, antifungal and cytotoxic properties of some sulfonamide incorporated ferrocenes//*Journal of Enzyme Inhibition and Medicinal Chemistry.* - 2009. - Vol. 29. - №1. - P. 169-175.

23. Умаров Б.Б., Сулаймонова З.А., Тиллаева Д.М. Комплексные соединения переходных металлов на основе конденсации производных ферроцена с гидразидами карбоновых кислот. *Научный вестник Наманганского государственного университета*, 2020.- Выпуск: 9. - С. 58-63.

24. Умаров Б.Б., Сулаймонова З.А., Ачылова М.К. Синтез комплексов на основе монокарбонильных производных ферроцена с гидразидами карбоновых кислот // *Universum: Химия и биология: электрон. Науч. Журн.* - 2021.-№1(79).-С.85-91.URL:

[\(http://7universum.com/ru/nature/archive/item/category/179/\)](http://7universum.com/ru/nature/archive/item/category/179/).

25. Sulaymonova Z.A., Umarov B.B. Preparation of ferrocenoylacetone meta-nitrobenzoylhydrazone and syntheses based on it // *Chemical technology. Control and management.* - 2021. - No. 4 (100). - P. 5-11.